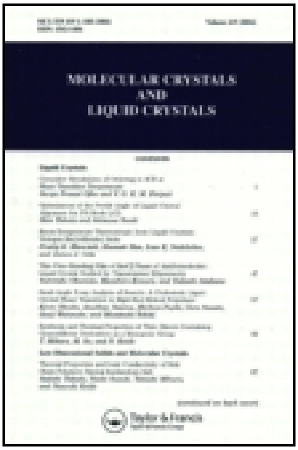

Molecular Crystals and Liquid Crystals
Publication details, including instructions for authors and subscription information:
http://www.tandfonline.com/loi/gmcl20

Dissipative Particle Dynamics Approach to Mesophase Formation and Behaviour

Alexandre E. Gomes [a], Assis F. Martins [a] & Antonino Polimeno [b]

[a] Depart. Ciência dos Materiais, Faculdade de Ciências e Tecnologia, Universidade Nova de Lisboa, Caparica, Portugal

[b] Dipart. di Scienze Chimiche, Università degli Studi di Padova, Padova, Italy

Version of record first published: 31 Aug 2006

To cite this article: Alexandre E. Gomes, Assis F. Martins & Antonino Polimeno (2005): Dissipative Particle Dynamics Approach to Mesophase Formation and Behaviour, Molecular Crystals and Liquid Crystals, 435:1, 135/[795]-152/[812]

To link to this article: http://dx.doi.org/10.1080/15421400590954858

Mol. Cryst. Liq. Cryst., Vol. 435, pp. 135/[795]–152/[812], 2005
Copyright © Taylor & Francis Inc.
ISSN: 1542-1406 print/1563-5287 online
DOI: 10.1080/15421400590954858

Dissipative Particle Dynamics Approach to Mesophase Formation and Behaviour

Alexandre E. Gomes
Assis F. Martins
Depart. Ciência dos Materiais, Faculdade de Ciências e Tecnologia,
Universidade Nova de Lisboa, Caparica, Portugal

Antonino Polimeno
Dipart. di Scienze Chimiche, Università degli Studi di Padova,
Padova, Italy

We have proposed recently to extend the use of the Dissipative Particle Dynamics (DPD) technique to the study of anisotropic mesophases, following its proven effectiveness in describing isotropic complex fluids. This technique circumvents, at least in part, the serious limitations on time-scales and physical dimensions inherent to molecular modelling simulations, e.g. Molecular Dynamics (MD) and Monte Carlo (MC) techniques. In this work some preliminary results for systems made up of single mesogenic units are presented, including examples of formation of nematic phases. The reorientation process of mesogenic DPD chains under the influence of an external field and of shearing stresses are explored as illustrative cases. Once the methodology for generating mesogenic units is well implemented it will be possible to use these units as building blocks for more complex structures like polymer liquid crystals or liquid crystalline suspensions of short fibers in a polymeric matrix.

Keywords: dissipative particle dynamics; DPD; mesophase; nematic phase

This work was partly supported by the Fundação para a Ciência e a Tecnologia, Portugal, through the research grant SFRH/BD/2982/2000 to A.E. Gomes and research project POCTI/CTM/2329/01.

Address correspondence to Prof. A. Farinha Martins, Dpt. Ciência dos Materiais, Faculdade de Ciências e Tecnologia, Universidade Nova de Lisboa, 2829-516 Caparica, Portugal. E-mail: asfm@fct.unl.pt

1. INTRODUCTION

Numerical and computational methodologies are by now well established in the interpretation of physical properties of complex fluids. They are useful in simulating static and dynamic properties with varying degrees of accuracy and different space and time scales. The use of such tools allows one to investigate from atomic level detail to macroscopic sample dimensions, and helps in the validation of theoretical models, their confrontation with experimental data, and the optimization of parameters. Various computational techniques have been employed for the study of liquid crystals since the anisotropic interaction potentials defined by Lebwhol-Lasher (LL) in the early 70's [1] were used to compute the nematic order parameter [2,3]. Recently, Molecular Dynamics (MD) and Monte Carlo (MC) techniques were successfully applied to oriented polymers [4], and full molecular simulations, based on atomistic potentials, were reported in the literature [5]. Nevertheless, the level of detail of molecular modelling in MD or MC simulations represents a significant burden on the maximum time evolution and physical dimensions allowed, which can hardly be extrapolated to the values required for direct interpretation of data from complex experimental set-ups used in rheological experiments. More recently, coarse-grained techniques based on lattice bond fluctuation models [6], smoothed particle hydrodynamics (SPH) [7] and dissipative particle dynamics (DPD) [8,9] emerged as useful tools for dealing with large size samples, at least in the case of isotropic fluids. In this paper we discuss an application of DPD to anisotropic media, in order to demonstrate the potential usefulness of this technique in the field of computational rheology of liquid crystals.

2. DPD METHODOLOGY

The DPD methodology was initially developed in 1992 by Hoogerbrugge and Koelman [8] for the study of the dynamic behaviour of complex fluids, and is based on well-proven molecular dynamics algorithms [10] that are comparatively much simpler and faster than the computational fluid dynamics codes usually employed in the analysis of problems of macroscopic scale. The particles used in the simulations are of mesoscopic dimensions, and can be regarded as groups of atoms or patches of fluid (*DPD beads*). In a typical DPD run, particles move according to Newton's laws of motion and interact via simplified force laws. The forces acting on each particle result from interactions with the neighboring particles and from additional body forces, e.g. those due to magnetic fields. Interactions are pair-wise and vanishing when the distance between beads are beyond a given *cut-off radius*. The particle-particle potential is chosen to reflect the interaction between patches of fluid, which can interpenetrate each other during the simulation.

The DPD approach was originally developed for describing isotropic phases. In a previous work [11] we have proposed an extension of this technique to study liquid crystalline phases. This was achieved through the definition of *DPD mesogenic units* and the use of an extension of the DPD technique to polymeric systems [12,13], resulting in a simple approach to the modulation of main-chain thermotropic nematic polymers.

The computational implementation follows closely the traditional MD scheme, starting with the description of the dynamical behaviour of particles, which move according to Newton's law of motion:

$$\begin{aligned} \frac{d\mathbf{r}_i}{dt} &= \mathbf{v}_i \\ m_i \frac{d\mathbf{v}_i}{dt} &= \boldsymbol{f}_i \end{aligned} \tag{1.1}$$

where $\boldsymbol{r}$ represents the particle position, m the particle mass, $\boldsymbol{v}$ its velocity, and $\boldsymbol{f}$ the force acting on it; the index i runs over all the particles. The basic forces acting on the particles are soft repulsion forces, pair-wise dissipation forces and pair-wise random forces. Those are the classical forces used by Hoogerbrugge and Koelman, and are to be formulated as simple as possible. Additional conservative forces can be added to complete the model, such as: bead-to-bead (polymeric) spring forces, orienting potentials, etc.

The typical repulsive forces used are derived from a soft interaction potential,

$$U_C = \begin{cases} \alpha \frac{a r_c}{2} \left(1 - \frac{r}{r_c}\right)^2 & \text{for } r < r_c \\ 0 & \text{for } r > r_c \end{cases} \tag{1.2}$$

where a is the force parameter setting the overall strength of repulsion, α is a dimensionless parameter that measures the relative repulsion strength when different bead species are present, r_c is the already mentioned cut-off radius and r is the distance between the particles. This potential produces a *conservative force* of the form:

$$\begin{aligned} f_c &= \alpha a \cdot w_C \\ w_C(r) &= \begin{cases} (1 - \frac{r}{r_c}) & \text{for } r < r_c \\ 0 & \text{for } r > r_c \end{cases} \end{aligned} \tag{1.3}$$

The *dissipative force* is defined as acting between each pair of particles in a way that reduces their relative velocity:

$$f_D = -\gamma w_D(r) v^{\|}$$
$$w_D(r) = w_C(r)^2 = \begin{cases} (1 - \frac{r}{r_c})^2 & \text{for } r < r_c \\ 0 & \text{for } r > r_c \end{cases} \tag{1.4}$$

where $v^{\|}$ is the relative velocity along the line joining the centers of mass of the particles. The strength of the dissipative interaction is given by γ. A matching *random force* acts on the particles according to a fluctuation-dissipation relationship:

$$\begin{aligned} f_R &= -\sigma\xi(t) w_R(r) \\ w_R(r) &= w_C(r) \end{aligned} \tag{1.5}$$

The relevant parameters of the random and dissipative forces, σ and γ, are mutually defined by the expression: $\sigma^2 = 2\gamma k_B T$ which relates the two parameters through the temperature of the system. $\xi(t)$ stands for a *white noise* random function. It has been shown that under these assumptions the equilibrium state of the system is a canonical (Maxwell–Boltzman) distribution, determined by the conservative forces (soft repulsions and other forces eventually acting on the particles), with the temperature being fixed by the balance between the dissipative and random forces [14].

The integration algorithm for the DPD equations of motion is not straightforward, given that the dissipative forces term involve the velocities of the particles. Our method of integration is based on a second order scheme analogous to the Verlet leapfrog algorithm [9]:

$$\begin{aligned} \boldsymbol{r}_i(t + \Delta t) &= \boldsymbol{r}_i(t) + \Delta t \times \boldsymbol{v}_i(t) + \frac{1}{2}\Delta t^2 \boldsymbol{f}_i(t) \\ \tilde{\boldsymbol{v}}_i(t + \Delta t) &= \boldsymbol{v}_i(t) + \frac{1}{2}\Delta t \times \boldsymbol{f}_i(t) \\ \boldsymbol{f}_i(t + \Delta t) &= \boldsymbol{f}_i(\boldsymbol{r}_i(t + \Delta t), \tilde{\boldsymbol{v}}_i(t + \Delta t)) \\ \boldsymbol{v}_i(t + \Delta t) &= \boldsymbol{v}_i(t) + \frac{1}{2}\Delta t[\boldsymbol{f}_i(t) + \boldsymbol{f}_i(t + \Delta t)] \end{aligned} \tag{1.6}$$

All DPD simulations made use of reduced units of mass, length and force, represented here by m, r_c and a. In the more usual cases all the DPD particles are considered to possess equal mass, m, which is chosen equal to 1 and is usually not explicit in the description of the DPD formalism. The reduced parameters are defined as $T^* = k_B T / a r_c$

$K^* = kr_c/a$, $\gamma^* = \gamma\sqrt{r_c/ma}$, and $\sigma^* = \sqrt{2T^*\gamma^*}$. Further details about the simulation and parameters used are given in [9,11].

Polymeric Chains in DPD

A polymeric chain is usually defined for the DPD simulations through a bead-spring model [12], the elastic force between contiguous DPD beads being given by:

$$k(r_{ij} - r_{eq}) \tag{1.7}$$

where k is the entropic spring elastic constant (Hooke's law), r_{ij} the distance between the two connected beads and r_{eq} the equilibrium distance for the spring, that is, the distance for which the elastic force is null. Polymeric systems can be described by this simple model, with the advantage that each chain can be represented by a relatively small number of beads [9,12,13], typically ranging from 20 to 50.

Orienting Units in DPD

A liquid crystal polymer is formed by groups of orienting (mesogenic) units plus non-orienting units. For instance, a main-chain liquid crystal polymer can be modelled as a collection of mesogenic units connected by flexible spacers, as shown in Figure 1. In DPD, MD, MC, etc., orientational order will be generated in the liquid phase (represented by a collection of chains) as a result of the inclusion of ordering units. To build up DPD mesogenic units, one can consider long chains of DPD beads where one or several chain segments have a rigid or semi-rigid behaviour, induced by an extra elastic force acting only on the two terminal DPD beads of that or those segments and with an equilibrium distance equivalent to the full length of the segments being considered (cf. Fig. 2).

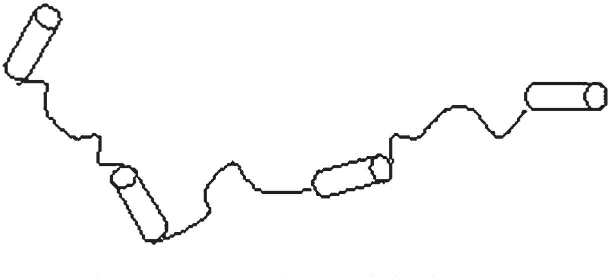

FIGURE 1 Main-chain nematic polymer. Cylinders represent the nematogenic units, and curved lines stand for the flexible parts of the chains.

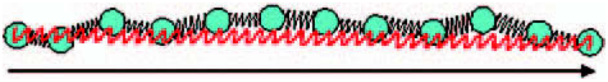

FIGURE 2 Representation of a semi-rigid chain of 12 DPD beads. All the beads and segments are defined according to the standard DPD procedures. The length of the semi-rigid segment and its rigidity, controlled by the external spring, confers the mesogenic properties.

Orientation by an External Field

To reproduce the orientational behaviour caused by an external field an appropriate potential is imposed on the system. We choose a P_2 potential acting on the vectors connecting the ends of the mesogenic units, whose strength is represented by the parameter ε_{ext}:

$$U_{ext} = -\varepsilon_{ext} P_2 = -\frac{\varepsilon_{ext}}{2}\left(3\cos^2\theta_i - 1\right) \tag{1.8}$$

where θ_i is the orientation angle between the mesogenic segment and the direction of the external field.

3. RESULTS

For the present study, a DPD system consisting of N chains (N changes according to the special case being considered) was computer generated. The parameters used in the DPD simulation are reported in Table 1 and are partly quoted from Groot and Warren [9]. The parameters

TABLE 1 DPD Simulation Parameters used in the Simulation of the Standard Rigid Segments. The * Means Scaled (Adimensional) Quantities

Bead-to-bead interaction parameter α	25
Random interaction parameter σ^*	3
Dissipative interaction parameter γ^*	18
Temperature, in reduced energy units, T^*	0.25
Bead-to-bead elastic constant k^*	100
Bead-to-bead elastic equilibrium distance	r_c
External elastic constant k_e^*	1000
External elastic equilibrium distance	$(n-1)\ r_c$
Number of beads per chain	n (1)
Number of chains	N (1)

(1) n and N take different values according to the experiment that is simulated.

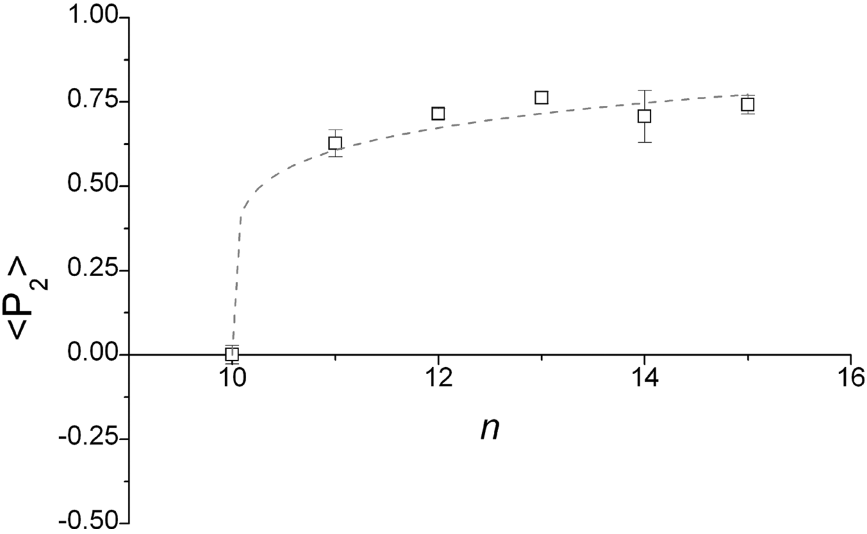

FIGURE 3 Internal order parameter $\langle P_2 \rangle$ as function of the number of DPD beads in a semi-rigid chain.

referring to the elastic connections have been determined in a previous work [11] and optimized to give good mesogenic properties to our DPD chains. The simulations were performed on a cubic cell with scaled dimension $L = 17.5\ r_c$ [10], using periodic boundary conditions. The system defined this way was used in all our simulations, unless stated otherwise.

To study the formation of ordered phases in the absence of an external field, a system consisting of 1,000 DPD beads characterized by the parameters in Table 1 was left free to evolve under the influence of internal forces. The procedure for testing the existence of ordered phases was as follows: the samples were initially prepared totally aligned with the $\hat{e_1}$ direction and very small random deviations were introduced on a bead-to-bead basis to avoid reaching a metastable situation. When the simulation started, the system was allowed to reach equilibrium in the absence of external fields and the simulation run long enough so as to achieve either an oriented or an isotropic stable arrangement. The order parameter values $\langle P_2 \rangle$ computed after an equilibrium state was reached are reported in Figure 3, in function of the number of beads, n, for a value of $T^* = 0.25$.

From Figure 3 it is possible to conclude that, for the set of parameters summarized in Table 1, chains of less than 11 beads do not show an ordered state. For $n = 11$ the order parameter $\langle P_2 \rangle$ assumes

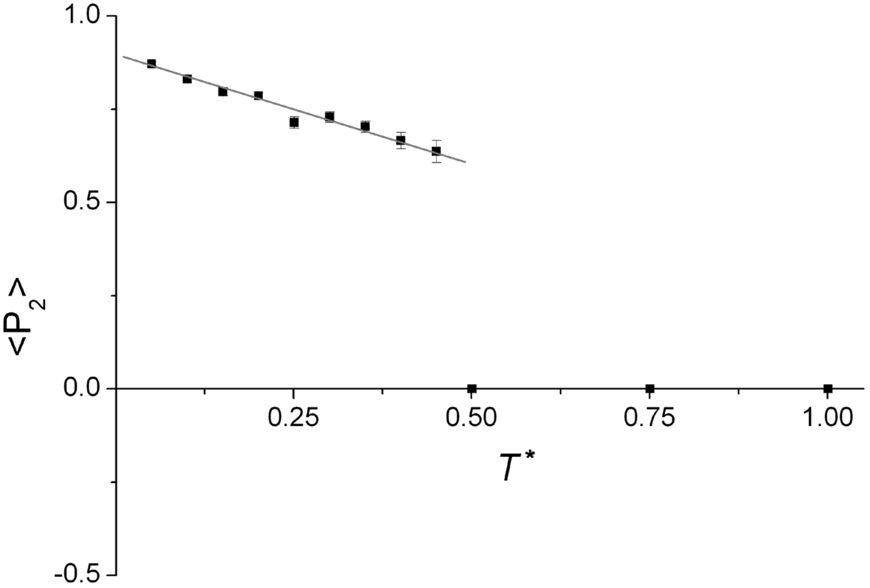

FIGURE 4 Equilibrium value of the internal order parameter $\langle P_2 \rangle$ for a system of 1,000 semi-rigid chains of 12 DPD beads at different temperatures (T^*).

the value 0.6 and for longer chains a slight increase of order is observed with increasing number of beads.

The 12-beads system is chosen as our reference system. We study the influence of the thermodynamic temperature, T^*, on the order of the system. In Figure 4 we show the order parameter for a system made of 1,000 chains of 12 DPD beads each, at various values of T^*: a phase transition between an ordered nematic state and an isotropic one can be observed between 0.45 and $0.5T^*$. The order parameter decreases with increasing temperature, as expected for the nematic phase, and vanishes in the isotropic phase.

Reorientation Under an External Field

A classical rheological experiment with liquid crystals, i.e. the observation of the collective reorientation of the molecules under the influence of an external field, was used as an illustrative application of the method. To simulate this case we used a system of 5,000 semi-rigid chains of 12 DPD beads each in a cubic cell of dimension $L = 30\,r_c$. To monitor the system evolution, two order parameters were recorded: an internal order parameter, defined with respect to the angles formed by the end-to-end vectors of each chain with the alignment direction, and a field order parameter, defined with respect to the initial orientation of the external field. Starting from an equilibrium configuration the system was left free for a short time to eliminate any numerical instabilities resulting from restarting the simulation. Then an external field was applied along the $\hat{e_1}$ direction and the system was left under its influence. Finally, after a long enough time to allow for the full orientation of the system, the external field was instantaneously switched on along an orthogonal ($\hat{e_3}$) direction and the reorientation process under the influence of the field was recorded. With field intensity equal to 0.05 a slight increase of the order was observed when the external field was first applied, followed by a decrease of the internal order parameter when the field was switched on along the orthogonal direction, i.e. during the reorientation process; finally the system realigned completely with the new field direction (cf. Fig. 5).

Three-dimensional snapshots of some of the most representative steps of the reorientation process are presented in Figure 6.

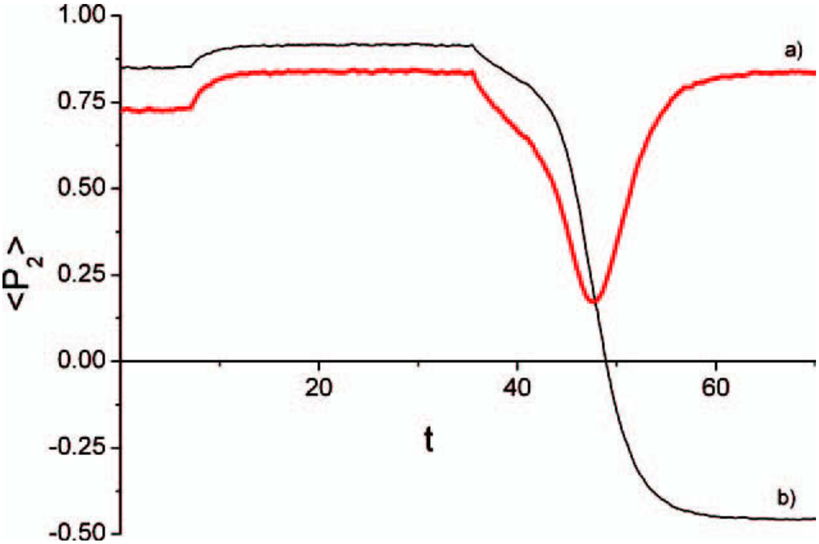

FIGURE 5 Time evolution of the order parameter $\langle P_2 \rangle$ for a system of 5,000 chains of 12 DPD beads under a switching external field: a) Order parameter with respect to internal preferred orientation; b) Order parameter with respect to the initial field orientation axis $\hat{e_1}$.

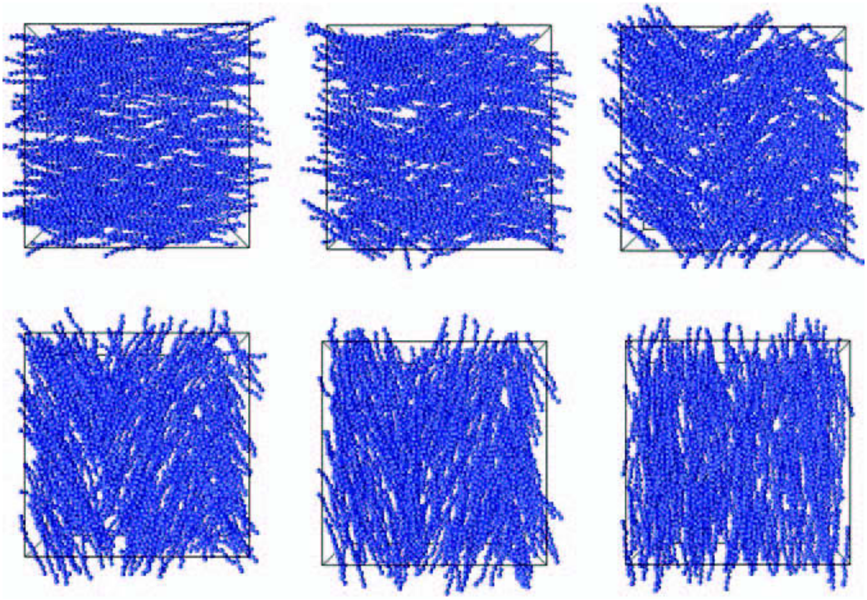

FIGURE 6 Snapshots of a system of chains of 12 DPD beads under a switching field, in chronologic sequence from initial configuration, on top left, to the final one, bottom right.

LCP Models from Standard Semi-Rigid DPD Systems

Using the same methodology it is possible to simulate longer chains and model liquid crystalline olygomeric and, eventually, polymeric (LCP) systems. Here we have dealt with a system of 40-beads chains, consisting of three semi-rigid segments of twelve beads each, linked by short flexible segments with two beads. The system was formed by 1,500 such chains, making a total of 60,000 beads, as in the previous case. The two systems have thus the same density, allowing a direct comparison. The alignment of the sample in the absence of external fields was verified in this case by the procedure already used for the system of 12-beads chains. The final equilibrium value of $\langle P_2 \rangle$ was found slightly smaller (0.68) than the one obtained for the previous system (0.74). One can notice that the longer chains take longer times to achieve a stationary situation. In Figure 7 we can observe the evolution of the order parameter for the two systems until equilibrium is reached, in the absence of an external field.

A switch experiment has also been performed, with the external field (derived from the potential (1.8)) applied in the usual way and

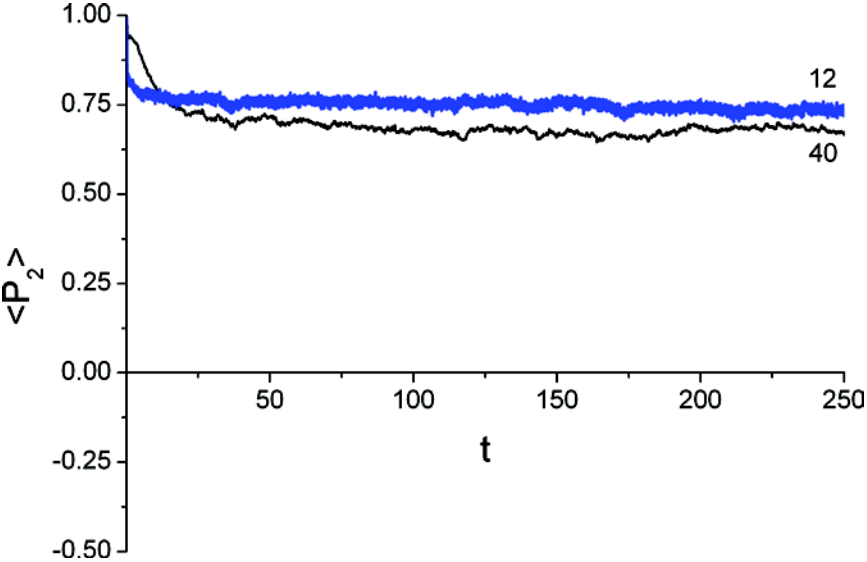

FIGURE 7 Orientation order parameter $\langle P_2 \rangle$ for two systems of semi-rigid chains of DPD beads: 12 beads chains (thick line) and longer chains of 40 beads grouped on 3 semi-rigid segments of 12 beads each (thin line).

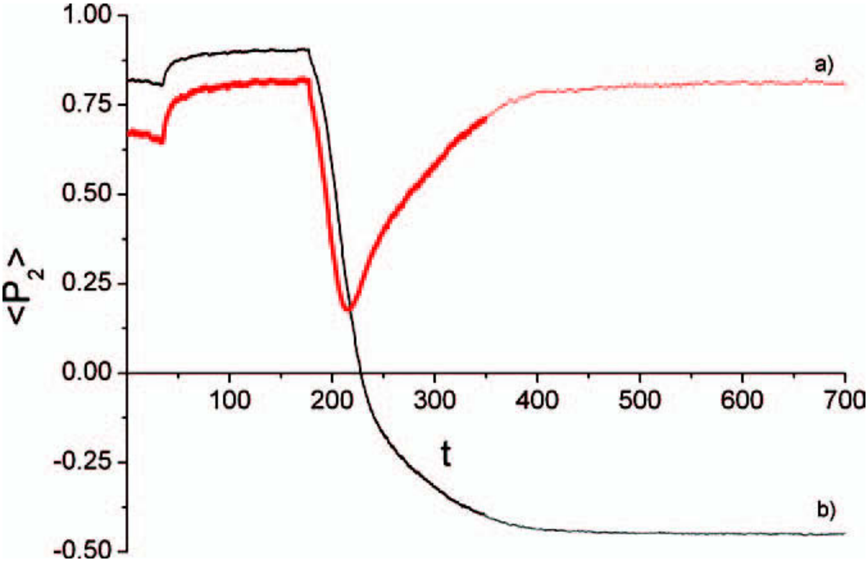

FIGURE 8 Time evolution of the orientation order parameter $\langle P_2 \rangle$ for a system of 1,500 chains of 40 DPD beads under a switching external field: a) Order parameter with respect to internal preferred orientation; b) Order parameter with respect to the initial field orientation axis $\hat{e_1}$.

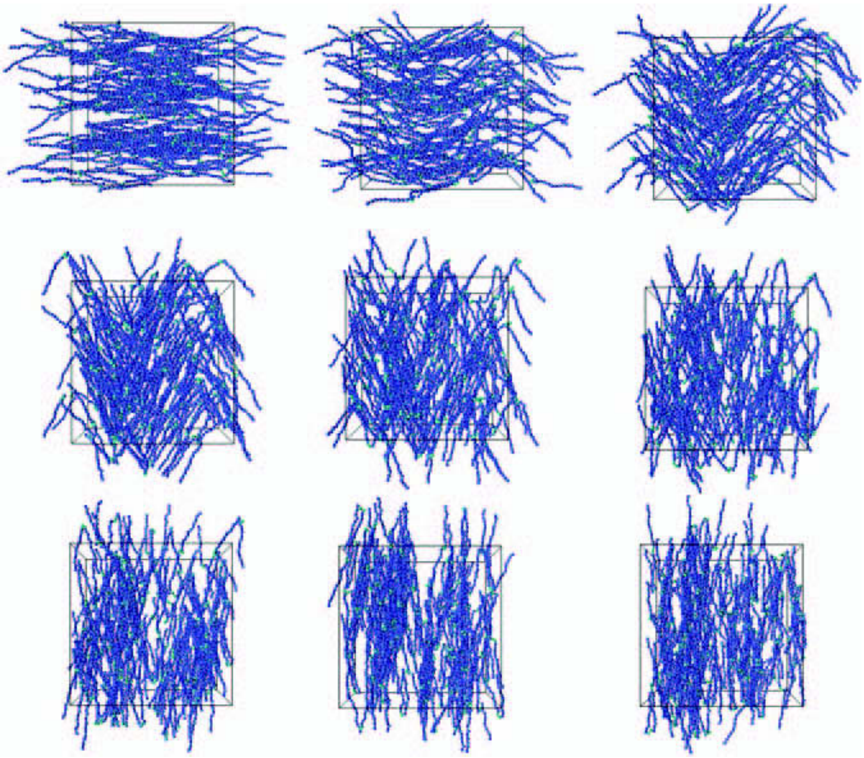

FIGURE 9 Snapshots of a system of chains of 40 DPD beads under a switching field, in chronologic sequence from initial configuration, on top left, to the final one, bottom right.

acting on the end-to-end vectors of the semi-rigid sections of the chain. The relative strength of the field was again 0.05. From the time evolution of the order parameter it can be seen that the reorientation process takes a significantly longer time (cf. Fig. 8 vs. Fig. 5). This fact can be qualitatively understood in terms of the lower mobility of the long chains; this can be directly observed on the sample snapshots presented in Figure 9.

Reorientation Under Shear

As a further example of the application of the DPD methodology, another typical rheological experiment was chosen, the shear flow of a mesomorphic material between parallel plates (Plane Couette flow). This simulation gives rise to further complexities, due to the necessary inclusion of a velocity field gradient in the DPD system. This is a problem well studied in MD simulations, and it is usually solved using the Lee-Edwards boundary condition [10], where the beads velocities in the repeating cells along a direction perpendicular to the velocity field are modified according to the imposed velocity profile. In DPD, another possible approach consists in introducing the representation of solid walls in the simulation, and imposing the desired velocity to the walls. In this work we decided to use the latter method, representing the walls according to the methodology proposed by Willemsen [15], since this technique presents the lower density fluctuations near the confining walls. Simulations with 36,000 beads were made, in a $5L \times 5L \times L$ box. Periodic boundary conditions were imposed on the $\hat{e_1}$ and $\hat{e_2}$ boundaries; the shear walls were implemented along the $\hat{e_3}$ boundary. The top wall moved at a prescribed velocity while the lower one remained at rest. The two model systems described previously,

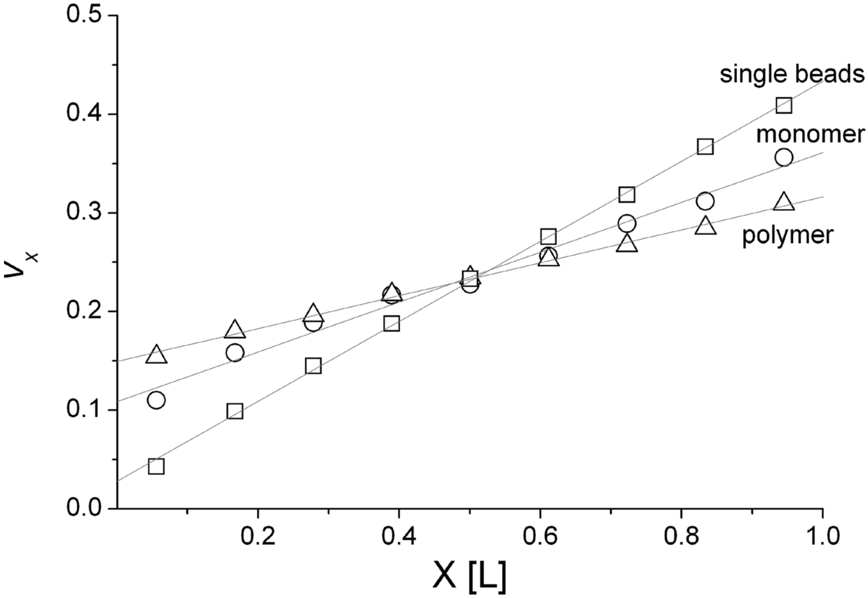

FIGURE 10 Average velocity profile after the equilibration stage on a $5 \times 5 \times 1$ slab DPD experiment. Velocities are plotted for: single DPD beads (squares), 12-beads “monomers” (circles) and 40-beads “polymers” consisting of three “monomers” freely connected through two beads (triangles). The increase of the walls-slip as the chains grow longer is noticeable.

consisting of 12-beads "monomers" (3,000 chains present) and 40-beads "polymers" (900 chains), have been tested. For comparison, we have also performed a simulation on a system of 36,000 free beads.

A significant problem posed by the wall construction in DPD is the so called velocity slip in the region near the walls: due to the lack of continuity of the velocity profile over the constructed walls, close to these the velocity will never be equal to the imposed value. Willemsen *et al*. [15] have designed and implemented an original methodology to minimize this problem, but, as it can be seen from Figure 10, the perfect adherence of the beads to the walls is never achieved. The slip phenomenon aggravates as the chains become longer, due to the fact that all beads of a given DPD chain are linked together and therefore move at approximately the same speed. Given that each bead will accelerate or decelerate all the other beads belonging to the same chain, the individual beads velocity will deviate from the one determined by the velocity profile.

In this preliminary study we were mainly interested in showing the influence of the shear rate on the dynamics of the orientation process.

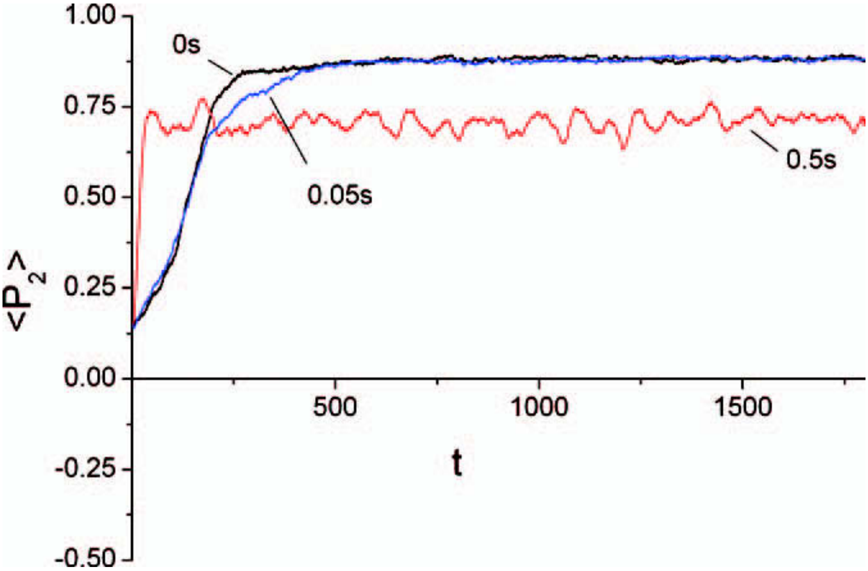

FIGURE 11 Time evolution of the orientation order parameter $\langle P_2 \rangle$ of a system of 3,000 chains of 12 DPD beads under shear. Order parameter computed with respect to the $\hat{e}_1$ axis (shear direction) for shear rates: 0, 0.05 and 0.5.

The samples were prepared in a form slightly different from the previous cases: the chain directions were randomly distributed in the $[\hat{e_1}, \hat{e_2}]$ plane and a random tilt was imposed in the $\hat{e_3}$ direction, taking care that the chains always remained confined between the shear planes. This initial configuration already showed a small degree of order, as can be verified from the initial value of the order parameter, $\langle P_2 \rangle = 0.14$. The time evolution of the order parameter is plotted in Figure 11. A large final order parameter was achieved, $\langle P_2 \rangle = 0.88$, with almost no fluctuations. For the highest shear rates the behaviour was slightly different: even if a high order parameter was achieved, it is significantly smaller (0.70) than the one obtained for low or vanishing shear rates. A completely stable state was never achieved, and there are significant oscillations of the order parameter. On the other hand, the transition time from a non ordered state to an ordered one is

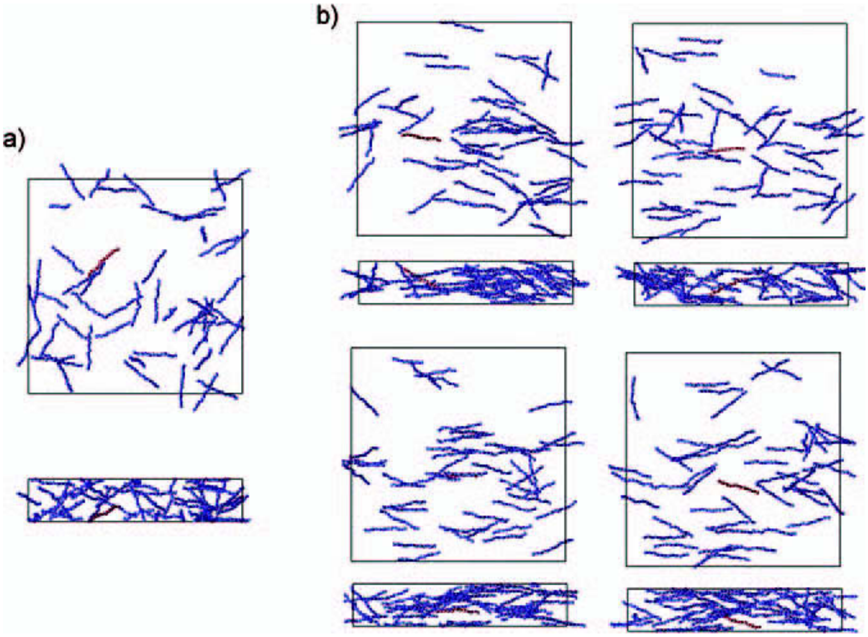

FIGURE 12 Top and lateral view of three-dimensional snapshots of a system chains of 12 DPD beads under constant shear: a) initial isotropic configuration (shear = 0); b) four snapshots, displayed chronologically from top-left to bottom-right, for the higher shear rate (0.5). For the sake of clarity, only 50 chains, out of 3,000, are represented.

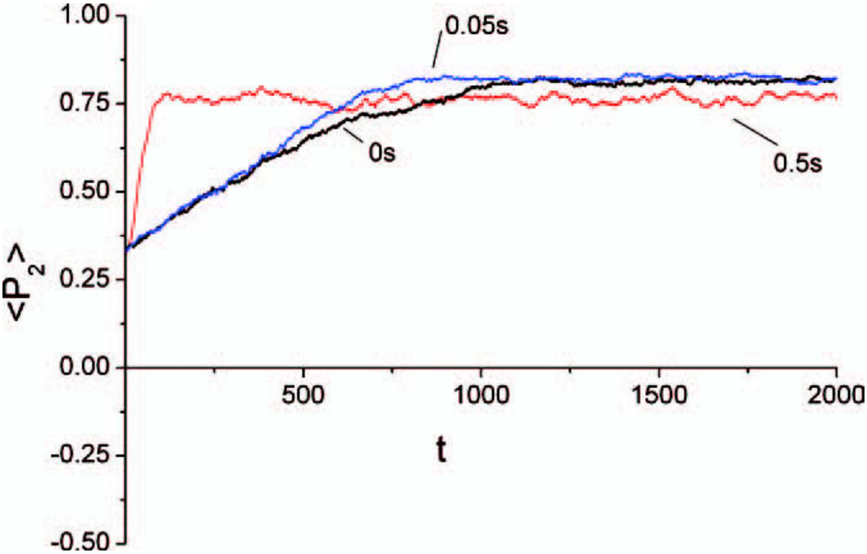

FIGURE 13 Time evolution of the orientation order parameter $\langle P_2 \rangle$ for a system of 900 "polymer" chains of 40 DPD beads (three 12-beads "monomers") under shear. Order parameter computed with respect to the $\hat{e_1}$ axis (shear direction) for shear rates: 0, 0.05 and 0.5.

lower in the higher shear rate case, meaning that the shear helps inducing nematic order.

The preceding remarks and the observation of the 3D snapshots of Figure 12 suggest that at high shear rates the chains have an oscillating behaviour. This cannot be considered a true tumbling, given that the inter-wall distance is not enough to allow the chains to perform a full rotation. Notice that in these snapshots only 50 out of the 3,000 chains present are shown. One chain has been singled out for better visualizing the dynamic evolution of the system.

The same procedure has been applied to the system of chains with 40 beads. In this case the transition time between the two ordered states, before and after the reorientation, increases significantly, as well as the difference in the time scales between the evolutions at the low and high shear rates. On the other hand, the difference between the final values of $\langle P_2 \rangle$ for the low (0.81) and high (0.76) shear rate regimes are not very pronounced, the stationary regime of the high shear rate case being more stable (cf. Fig. 13). The increased chain length, resulting in a higher resistance to the flow can explain this. Some relevant 3D snapshots for this case are exhibited in Figure 14.

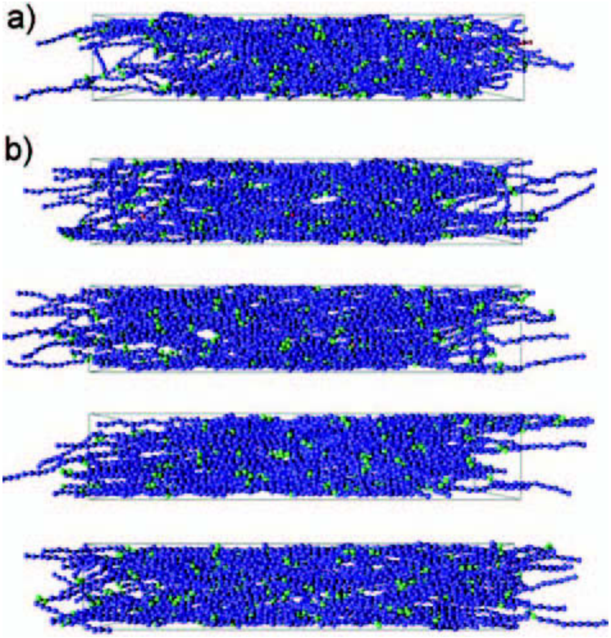

FIGURE 14 Snapshots of a system chains of 40 DPD beads under constant shear: a) initial isotropic configuration (shear = 0); b) four snapshots, displayed chronologically from top to bottom, for the higher shear rate (0.5). For the sake of clarity, only 100 chains, out of 900, are represented.

4. CONCLUSION

A DPD methodology to describe polymeric liquid crystals is proposed, which uses a representation based on chains of beads connected through elastic forces. Mesogenic units are represented by semi-rigid segments of the chain. This requires the implementation of external springs controlling the chain rigidity, can be done easily within the standard coarse-grained formulation of the DPD chains, and imposes little additional burden on the standard DPD approach for isotropic fluids. The mesogenic units can be taken individually (in the case of low molecular weight liquid crystals) or integrating longer DPD chains (in the case of polymeric liquid crystals). The main drawback of the method is that it requires a relatively high number of DPD beads to represent a single mesogenic unit; this problem may become critical when simulating long polymer systems.

Complex molecules can be represented through appropriate ramification of the bead-to-bead connections, so that the methodology can be easily extended to represent ramified polymers and even cross-linked polymers or elastomeric phases.

Test cases have been presented for the simulation of a few simple rheological experiments. Our results are in reasonable qualitative agreement with the known data obtained in laboratory experiments.

REFERENCES

[1] Lebwohl, P. A. & Lasher, G. (1972). *Phys. Rev.*, *A 6*, 426.
[2] Luckhurst, G. R. & Simpson, P. (1982). *Mol. Phys.*, *47*, 251.
[3] Fabbri, U. & Zannoni, C. (1986). *Molec. Phys.*, *58*, 763.
[4] Clarke, J. H. R. (1997). In: *The Physics of Glassy Polymers*, Young, R. J. & Haward, R. N. (Eds.), Chapman and Hall: London, UK, 33.
[5] Cook, M. J. & Wilson, M. R. (2001). *Mol. Cryst. Liq. Cryst.*, *363*, 181.
[6] Binder, K. & Paul, W. (1997). *J. Polym Sci. Part B – Polym. Phys.*, *35*, 1.
[7] Español, P. (1997). *Europhys Lett.*, *39*, 605.
[8] Hoogerbrugge, P. J. & Koelman, J. M. V. A. (1992). *Europhys. Lett.*, *19*, 155; Koelman, J. M. V. A. & Hoogerbrugge, P. J. (1993). *Europhys. Lett.*, *21*, 363.
[9] Groot, R. D. & Warren, P. B. (1997). *J. Chem. Phys.*, *107*, 4423.
[10] Allen, M. P. & Tildesley, D. J. (1987). *Computer Simulation of Liquids*, Claredon Press: Oxford, U.K.
[11] Polimeno, A., Gomes, A. E., & Martins, A. F. (2004). In: *Computer Simulations of Liquid Crystals and Polymers*, Pasini, P., Zannoni, C., & Zumer, S. (Eds.), Kluwer: Dordrecht, 135.
[12] Schlijper, A. G., Hoogerbrugge, P. J., & Manke, C. W. (1995). *J. Rheol.*, *39*, 567.
[13] Kong, Y., Manke, C. W., Madden, W. G., & Schlijper, A. G. (1997). *J. Chem. Phys.*, *107*, 592.
[14] Español, P. & Warren, P. B. (1995). *Europhys Lett.*, *30*, 191.
[15] Willemsen, S. M., Hoefsloot, H. C. J., & Iedema, P. D. (2000). *Int. J. Mod. Phys.*, *C 11*, 881.